Self-consistent linear-optical response of thin metal films

A. V. Andreev* and A. B. Kozlov
Physics Department and International Laser Center, M. V. Lomonosov Moscow State University, Moscow 119899, Russia
(Received 3 June 2003; revised manuscript received 9 September 2003; published 11 November 2003)

The linear-optical properties of unbacked thin metal films are studied within the jellium model and the time-dependent density-functional approach. Unlike most previous calculations, the present ones treat both longitudinal and transverse components of electromagnetic fields microscopically and results are performed in terms of strictly calculated reflection, transmission, and absorption coefficients. Dependences of the collective mode frequencies on metal film thickness are discussed. It is shown that in thin metal film there are collective modes which can be interpreted as standing plasma waves. Also it is demonstrated that in thin metal films there exists a couple of surface modes which are related to the so-called multipole surface-plasmon mode. Spectral and angular dependences of optical response are discussed in detail. A few specific features of optical response under conditions of collective mode excitations have been found. In particular, metal film cannot absorb more than a half of energy flux of incident wave. At the angle of incidence, when absorption reaches the absolute maximum the reflection and transmission coefficients are equal to one-fourth. These and some other features appear in the same manner for different collective mode excitations. Also, we consider how the spectrum of collective mode excitations is transformed under the transition from two- to three-dimensional electron systems.

DOI: 10.1103/PhysRevB.68.195405 PACS number(s): 78.67.De, 73.21.Fg, 71.15.Mb, 78.20.Bh

I. INTRODUCTION

In the present work we study the linear-optical response of unbacked thin metal films to the applied field of plane electromagnetic wave. We consider thin metal films which represent so-called two-dimensional (2D) electron systems. In such systems the motion of electrons is quantized in one direction and free in two others. 2D electron systems have been studied for many years[1] and they are also realized in, for example, semiconductor quantum wells, inversion layers, heterostructures, and on the surface of liquid helium.

When we treat the optical response of thin metal films it is necessary to keep in mind the following two things. First, the optical response of thin metal films is substantially nonlocal and cannot be adequately described in terms of a dielectric permittivity or multipole expansion of electronic response. Second, electrons in thin metal film interact with each other and the motion of any electron depends on the state of the whole electron system. The latter means that the optical response of thin metal films can be described only within the framework of self-consistent theory.

Electron excitations in 2D systems are of particular interest because they promise a great deal of possible applications. Traditionally, they are decomposed into two distinct categories:[2] single-particle and collective excitations. The single-particle excitations arise from transitions of an electron to the states that lie above the Fermi surface. In 2D electron systems there are intrasubband and intersubband single-particle excitations. The energies of these excitations are determined by the energy difference between the final and initial states of an electron. The concept of single-particle excitations is very important in solid-state plasma physics but it is rather an abstract concept because in reality it is impossible to excite one electron independently of others. In fact electrons interact with each other and as a result the collective excitations become dominant. The collective excitations arise from the coupling of the single-particle excitations. This coupling is due to the interaction of electrons with the self-consistent electromagnetic field produced by the whole electron system. The single-particle excitations can be coupled via the three different electric field components. If a 2D electron system interacts with an electric field perpendicular (parallel) to the surface of the 2D system, then we can speak about the longitudinal (transverse) collective excitations as in this limiting case the electric field is longitudinal (transverse). The longitudinal field is a gradient of a scalar function and divergence of the transverse field is equal to zero.

It is known that the coupling of the single-particle intersubband excitations via the electromagnetic field component parallel to the surface of 2D electron gas is extremely weak.[3] As a result the frequencies of transverse collective modes almost coincide with the single-particle intersubband transition frequencies. For thin metal film the difference between these frequencies is only about 10^{-5} eV, which is much smaller than the characteristic absorption linewidth. And so the transverse collective excitations are usually associated with the single-particle excitations. On the contrary, the longitudinal collective mode frequencies can be significantly shifted from the single-particle intersubband transition frequencies.[4–6] The shift between these frequencies arises from two contributions. The direct Coulomb interaction results in the depolarization shift and the exchange-correlation interaction gives the excitonic correction. Recently, both contributions have been extensively studied in semiconductors quantum wells.[7] The transverse and longitudinal collective modes can be considered separately only in the limiting cases, when the electric field is parallel or perpendicular to the surface of 2D electron gas. However, in the general case, they are coupled. There are a number of different mode-coupling effects. The coupling between the intrasubband and intersubband collective modes was studied in Refs. 8 and 9.

The resonant coupling between the single-particle and collective modes was considered in Ref. 2.

In this paper we use the jellium model to describe electron properties of thin metal films. Within the framework of this model the discrete charges of ions are replaced by a uniform positively charged background. Then the valence electrons are treated within the density-functional formalism.[10,11] The electron response of jellium films is usually calculated under the assumption that the transverse component of the electronic response is negligible.[12,13] This approximation considerably simplifies the procedure of calculation of the electronic response as the electromagnetic field can be characterized by only the scalar potential. One of the limitations of this approximation is that results of calculations are performed in terms of auxiliary quantities which cannot be directly measured in experiment. In the present work, both longitudinal and transverse components of the electromagnetic field are treated rigorously within the density-functional approach and results are presented in terms of the strictly calculated reflection, transmission, and absorption coefficients of thin metal film.

The outline of this paper is as follows: In Sec. II we discuss basic equations which determine the linear-optical response of thin metal films within the time-dependent density-functional theory. A method of their solution in a particular case of *s*-polarized incident wave is specified. In Sec. III we consider excitations of the longitudinal collective modes. Dependences of the collective mode frequencies on film thickness are discussed in detail. Reflection, transmission, and absorption spectra of thin metal film are considered in Sec. IV. The field distribution in thin metal film is discussed in Sec. V. The dependence of the optical response of thin metal film on the angle of incidence of the electromagnetic wave is analyzed in Sec. VI. In Sec. VII we consider the important question how 2D collective modes transform into 3D plasmons. Conclusions are given in Sec. VIII.

II. THEORY OF THE LINEAR-OPTICAL RESPONSE

A. Charge and current densities

In this subsection we derive expressions for the charge and current densities induced in the jellium film by an external field. The motion of electrons in the jellium film can be described by the Schrödinger-type equation

$$i\hbar\frac{\partial\Psi_j}{\partial t}=-\frac{\hbar^2}{2m_e}\vec{\nabla}^2\Psi_j+e\varphi\Psi_j+V\Psi_j+\frac{i\hbar e}{2m_ec}(\vec{\nabla}\vec{A}+\vec{A}\vec{\nabla})\Psi_j+\frac{e^2}{2m_ec^2}\vec{A}^2\Psi_j, \quad (1)$$

where φ and $\vec{A}$ are the field potentials, V is the exchange-correlation potential, and Ψ_j is the wave function of the jth electron. In the steady-state case Eq. (1) transforms into the Kohn-Sham equation.[11] We describe the exchange and correlation interaction between electrons by the scalar potential V. Strictly speaking, it is justified only if the jellium film interacts with the longitudinal electric field, while in general case the exchange and correlation effects must be described by the vector potential.[14–16] Nevertheless, we use the scalar potential V because we will mainly discuss the situations when the longitudinal part of electromagnetic field in the jellium film is significantly larger than the transverse part.

We consider the solution of Eq. (1) within the perturbation theory, assuming that the external field is much smaller than the internal field in the film. The wave function can be expanded into series

$$\Psi_j=\Psi_{0j}+\Psi_{1j}+\cdots, \quad (2)$$

where Ψ_{0j} is the wave function in the absence of external field, which can be written in the form

$$\Psi_{0j}(\vec{r},t)\rightarrow\Psi_{0n,\vec{k}_t}(\vec{r},t)=\frac{1}{\sqrt{S}}\exp\left(-\frac{i}{\hbar}E_{n,\vec{k}_t}t+i\vec{k}_t\vec{r}\right)\Phi_n(z). \quad (3)$$

Here, we assume that the state of the jth electron is characterized by the quantum number n and the tangential component of wave vector $\vec{k}_t$, z is the normal coordinate, and S is the area of film surface. The eigenvalues $E_{n,\vec{k}_t}$ is the sum of the energies of free longitudinal and quantized transversal motions,

$$E_{n,\vec{k}_t}=\frac{\hbar^2\vec{k}_t^2}{2m_e}+\varepsilon_n, \quad (4)$$

and the eigenfunctions Φ_n satisfy the one-dimensional Kohn-Sham equation

$$\frac{d^2\Phi_n}{dz^2}+\frac{2m_e}{\hbar^2}(\varepsilon_n-e\varphi_0-V_0)\Phi_n=0, \quad (5)$$

where $e\varphi_0$ and V_0 are the Hartree and local exchange-correlation potentials, respectively. To evaluate V_0 we use Wigner's formula for the exchange and correlation energy per particle of homogeneous electron gas.[17]

If the metal film interacts with a plane, monochromatic wave, then the potentials can be written in the form

$$\varphi(\vec{r},t)=\varphi_0(z)+\varphi_1(z)\exp(i\vec{q}_t\vec{r}-i\omega t)+\cdots, \quad (6a)$$

$$\vec{A}(\vec{r},t)=\vec{A}_1(z)\exp(i\vec{q}_t\vec{r}-i\omega t)+\cdots, \quad (6b)$$

$$V(\vec{r},t)=V_0(z)+V_1(z)\exp(i\vec{q}_t\vec{r}-i\omega t)+\cdots, \quad (6c)$$

where ω is the field frequency and $\vec{q}_t$ is the tangential component of wave vector. The complex amplitudes of potentials denoted by subscript 1 are assumed to be linear in amplitude of the incident wave and the complex amplitude for the charge and current densities,

$$\rho=e\sum_j|\Psi_j|^2, \quad (7a)$$

$$\vec{J}=-\frac{e}{m_ec}\vec{A}\rho+\frac{i\hbar e}{2m_e}\sum_j(\Psi_j\vec{\nabla}\Psi_j^*-\Psi_j^*\vec{\nabla}\Psi_j), \quad (7b)$$

can be introduced in the same way.

Substitution of Eqs. (2) and (6) into Eq. (1) with subsequent linearization gives an equation for Ψ_{1n}, which can be solved in the usual way—namely, by expanding Ψ_{1n} over the Kohn-Sham eigenfunctions Φ_n. In this expansion we take into account only the bound states; i.e., we neglect transitions of electrons from the states of discrete spectrum to the states of continuous spectrum. It should be noted that this approximation is justified only for analysis of the electron excitations with the energies that lie below the continuum threshold. The excitations with higher energies can be influenced by the electron transitions to the continuum states. For the sake of definiteness, let us choose a coordinate system so that $\hat{y}$-$\hat{z}$ is the plane of incidence. Straightforward calculation gives the following expressions for the complex amplitudes of charge and current densities:

$$J_{1x}=-\frac{e}{m_e c}\rho_0 A_{1x}-\frac{\hbar e^2 k_{F0}^4}{8\pi m_e^2 c}\sum_{n,m}\Phi_n\Phi_m^*[A_{1x}]_{nm}\frac{R_{1,nm}}{D_{nm}}, \tag{8a}$$

$$J_{1y}=-\frac{e}{m_e c}\rho_0 A_{1y}-\frac{e k_{F0}^3}{4\pi m_e}\sum_{n,m}\Phi_n\Phi_m^*\left([H_\parallel]_{nm}\frac{R_{2,nm}}{D_{nm}}-[e\varphi_1+V_1+H_\perp]_{nm}\frac{R_{3,nm}}{D_{nm}}\right), \tag{8b}$$

$$J_{1z}=-\frac{e}{m_e c}\rho_0 A_{1z}+\frac{ie k_{F0}^2}{4\pi m_e}\sum_{n,m}(\Phi_n\nabla_z\Phi_m^*-\Phi_m^*\nabla_z\Phi_n)\times\left([e\varphi_1+V_1+H_\perp]_{nm}\frac{R_{4,nm}}{D_{nm}}-[H_\parallel]_{nm}\frac{R_{3,nm}}{D_{nm}}\right), \tag{8c}$$

$$\rho_1=\frac{e k_{F0}^2}{2\pi\hbar}\sum_{n,m}\Phi_n\Phi_m^*\left([e\varphi_1+V_1+H_\perp]_{nm}\frac{R_{4,nm}}{D_{nm}}-[H_\parallel]_{nm}\frac{R_{3,nm}}{D_{nm}}\right), \tag{8d}$$

where

$$H_\parallel=\frac{\hbar e k_{F0}}{2m_e c}A_{1y},\quad H_\perp=\frac{i\hbar e}{2m_e c}(\nabla_z A_{1z}+A_{1z}\nabla_z), \tag{9}$$

$k_{F0}=(3\pi^2\bar{n})^{1/3}$, $\bar{n}$ is the density of the positive background, $D_{nm}=\omega_{nm}-\omega-i\gamma_{nm}$, $\hbar\omega_{nm}=(\varepsilon_n-\varepsilon_m)$ is the energy difference between the nth and mth eigenstates, and γ_{nm} is the phenomenologically introduced transverse relaxation rate. For the sake of simplicity we will assume further that the relaxation rate γ_{nm} does not depend on the initial and final states nth and mth—namely, $\gamma_{nm}=\tau^{-1}$ where τ is the transverse relaxation time. The square brackets in Eqs. (8) are used to denote the matrix elements—i.e., $[F]_{nm}=\int\Phi_n^* F\Phi_m dz$, where F is an arbitrary operator. Expressions (8) contain the dimensionless quantities

$$R_{p,nm}=\Theta_n\left(\frac{\varepsilon_F-\varepsilon_n}{\varepsilon_{F0}}\right)^{l_p}I_p\left(\frac{\hbar q_y k_{F0}}{m_e D_{nm}}\sqrt{\frac{\varepsilon_F-\varepsilon_n}{\varepsilon_{F0}}},-\frac{q_y}{2k_{F0}}\sqrt{\frac{\varepsilon_{F0}}{\varepsilon_F-\varepsilon_n}}\right)-\Theta_m\left(\frac{\varepsilon_F-\varepsilon_m}{\varepsilon_{F0}}\right)^{l_p}I_p\times\left(\frac{\hbar q_y k_{F0}}{m_e D_{nm}}\sqrt{\frac{\varepsilon_F-\varepsilon_m}{\varepsilon_{F0}}},\frac{q_y}{2k_{F0}}\sqrt{\frac{\varepsilon_{F0}}{\varepsilon_F-\varepsilon_m}}\right), \tag{10}$$

where $p=1,2,3,4$; $l_1=l_2=2$, $l_3=3/2$, $l_4=1$; $\Theta_n\equiv\Theta(\varepsilon_F-\varepsilon_n)$ is the Heaviside unit step function, $\varepsilon_{F0}=\hbar^2 k_{F0}^2/2m_e$, and ε_F is the Fermi energy. In its turn expression (10) includes the following integrals:

$$I_1(a,b)=\frac{8}{3\pi}\int_{-1}^{1}dx\frac{(1-x^2)^{3/2}}{1+a(x+b)}, \tag{11a}$$

$$I_2(a,b)=\frac{8}{\pi}\int_{-1}^{1}dx\frac{(1-x^2)^{1/2}(x+b)^2}{1+a(x+b)}, \tag{11b}$$

$$I_3(a,b)=\frac{4}{\pi}\int_{-1}^{1}dx\frac{(1-x^2)^{1/2}(x+b)}{1+a(x+b)}, \tag{11c}$$

$$I_4(a,b)=\frac{2}{\pi}\int_{-1}^{1}dx\frac{(1-x^2)^{1/2}}{1+a(x+b)}, \tag{11d}$$

which can be calculated analytically. For example, in the particular case $q_y=0$ we have $I_1=I_2=I_4=1$ and $I_3=0$.

The obtained expressions for current density (8) consist of two terms. The first term defines the local response of an electron subsystem and the second term defines the nonlocal one. The local response at some point depends on the strength of the field at the same point whereas the nonlocal response depends on the field distribution inside the film.

B. Self-consistent equations

Equations (8) determine the functional dependence of the charge and current densities on the field and exchange-correlation potentials. Now, in order to get set of the self-consistent equations it is necessary to supplement Eqs. (8) with equations for the field and exchange-correlation potentials. We use the following gauge condition on field potentials:

$$\varphi-\varphi_0=0, \tag{12}$$

where φ_0 is the unperturbed scalar potential. In other words the scalar potential φ does not depend on time and the linear response of the jellium film is fully determined by the vector potential $\vec{A}$. It can be shown that the equations for complex amplitudes of tangential and normal components of vector potential can be written in the form

$$\frac{d^2\vec{A}_{1t}}{dz^2}+q_z^2\vec{A}_{1t}=-\frac{4\pi}{c}\vec{j}_{1t}+\frac{4\pi c}{\omega}\vec{q}_t\rho_1, \tag{13a}$$

$$\frac{d^2A_{1z}}{dz^2}+q_z^2A_{1z}=-\frac{4\pi}{c}j_{1z}+\frac{4\pi c}{i\omega}\frac{d\rho_1}{dz}, \tag{13b}$$

where $\vec{j}$ is defined as

$$\vec{j}=\frac{e}{m_e c}\rho_0\vec{A}+\vec{J} \tag{14}$$

and

$$q_z^2(z)=\frac{\omega^2}{c^2}\varepsilon(z)-q_y^2, \tag{15}$$

$$\varepsilon(z)=1-\frac{4\pi e\rho_0(z)}{m_e\omega^2}. \tag{16}$$

The quantities q_z and ε should not be interpreted as the normal component of the wave vector and dielectric permittivity, respectively. In our calculations we use the adiabatic local-density approximation[18,19] for the induced exchange-correlation potential:

$$V_1=\frac{dV_0}{d\rho_0}\rho_1. \tag{17}$$

Here it should be noted that it is the simplest possible approximation. More sophisticated approximations have been extensively discussed recently.[15,16,20]

So we get the self-consistent equations (8), (13), and (17), which fully determine linear-optical response of thin metal films.

C. *s*-polarized incident wave

In this subsection we discuss the equation for the vector potential which describes the interaction of the jellium film with *s*-polarized incident wave. Substitution of Eq. (8a) into Eq. (13a) yields

$$\frac{d^2A_{1x}}{dz^2}+q_z^2A_{1x}=\frac{\hbar e^2k_{F0}^4}{2m_e^2c^2}\sum_{n,m}\Phi_n\Phi_m^*\frac{R_{1,nm}}{D_{nm}}[A_{1x}]_{nm}. \tag{18}$$

The solution of this equation can be performed with the help of the Green function. Let u and v be linear-independent solutions of the homogeneous equation

$$\frac{d^2A_{1x}}{dz^2}+q_z^2A_{1x}=0, \tag{19}$$

which correspond to two waves with unit amplitudes that are incident on metal film from opposite sides. Then the solution of Eq. (18) can be written as

$$A_{1x}(z)=A_0u(z)+\frac{\hbar e^2k_{F0}^4}{2m_e^2c^2w}\times\sum_{n,m}\frac{R_{1,nm}}{D_{nm}}[A_{1x}]_{nm}\left(u(z)\int_{-\infty}^{z}dz'v(z')+v(z)\int_{z}^{+\infty}dz'u(z')\right)\Phi_n(z')\Phi_m^*(z'), \tag{20}$$

where A_0 is the amplitude of vector potential of the incident wave and w is the Wronskian. The solution (20) contains the matrix elements $[A_{1x}]_{nm}$, which can be determined from the set of linear algebraic equations

$$[A_{1x}]_{kl}-\frac{\hbar e^2k_{F0}^4}{2m_e^2c^2w}\sum_{n,m}\frac{R_{1,nm}}{D_{nm}}[A_{1x}]_{nm}\left[\left(u(z)\int_{-\infty}^{z}dz'v(z')+v(z)\int_{z}^{+\infty}dz'u(z')\right)\Phi_n(z')\Phi_m^*(z')\right]_{kl}=A_0[u]_{kl}. \tag{21}$$

Finally, we note that the interaction of the metal film with *p*-polarized incident waves is described by three equations: for the tangential and normal components of the vector potential and for the induced exchange-correlation potential. These equations can be easily obtained as a result of substitution of Eqs. (8) into Eqs. (13) and (17). We do not discuss here these equations in detail, as their analysis is completely similar to that for the case of *s*-polarized incident waves.

III. LONGITUDINAL COLLECTIVE MODES

Before we proceed to a discussion of the linear-optical properties of thin metal films, we consider the solution of the self-consistent equations (8), (13), and (17) in the particular case of interactions of metal film with the longitudinal electric field. In order to keep this paper self-consistent we plot in Fig. 1 the dependences of eigenvalues ε_n and Fermi energy ε_F on jellium film thickness L. These dependences are calculated for the background density $\overline{n}$ characterized by the Wigner-Seitz radius $r_s(\overline{n})=4$ and they are needed for further analysis. We choose zero energy so that the electrostatic potential vanishes far from the metal film. In this case the work function is simply equal to the absolute value of the Fermi energy. It is seen from Fig. 1 that the Fermi energy exhibits oscillations. The period of these oscillations is very close to $\lambda_F/2\approx 0.35$ nm, where λ_F is the Fermi wavelength. These oscillations are connected with the appearance of new occupied subbands with increasing film thickness.

Let only the normal component of the vector potential be nonzero and depend only on the normal coordinate z. In this case the self-consistent equations (8), (13), and (17) can be solved.[5,6] For example, the solution for the vector potential is

$$A_{1z}=-i\frac{4ec}{\hbar\omega}\sum_{n>m}(\Phi_n\nabla_z\Phi_m-\Phi_m\nabla_z\Phi_n)\frac{R_{nm}^{(L)}}{\hbar\omega_{nm}}X_{nm}, \tag{22}$$

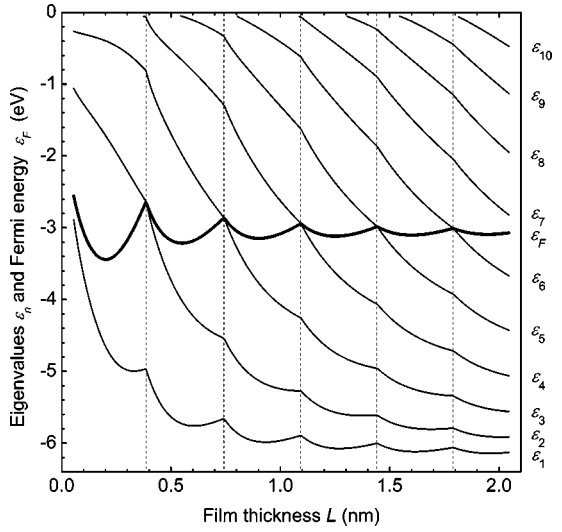

FIG. 1. Eigenvalues ε_n and Fermi energy ε_F vs metal film thickness L for $r_s(\bar{n})=4$. The dashed lines denote the film thicknesses at which new occupied subbands appear.

where

$$R_{nm}^{(L)}=\Theta_n(\varepsilon_F-\varepsilon_n)-\Theta_m(\varepsilon_F-\varepsilon_m) \tag{23}$$

and

$$X_{nm}=\frac{\omega_{nm}[V_1]_{nm}+\omega[H_\perp]_{nm}}{\omega_{nm}^2-\omega^2}. \tag{24}$$

Here, for the sake of simplicity, we assume that Φ_n are the real functions and we neglect the relaxation processes. In Eq. (22) we have omitted terms corresponding to the external field. The matrix elements X_{nm} can be found from the solution of the set of algebraic equations

$$\sum_{n>m} G_{kl,nm}X_{nm}=(\omega^2-\omega_{kl}^2)X_{kl}, \tag{25}$$

where

$$G_{kl,nm}=-\frac{R_{nm}^{(L)}}{\hbar\omega_{nm}}\left(\frac{2e^2}{m_e}\int(\Phi_k\nabla_z\Phi_l-\Phi_l\nabla_z\Phi_k)(\Phi_n\nabla_z\Phi_m-\Phi_m\nabla_z\Phi_n)dz+\frac{2m_e\omega_{kl}\omega_{nm}}{\pi\hbar^2}\times\int\Phi_k\Phi_l\frac{dV_0}{dn_0}\Phi_n\Phi_m dz\right). \tag{26}$$

The homogeneous system of coupled equations (25) has a nontrivial solution if its determinant is equal to zero. The frequencies of the longitudinal collective modes can be determined from this condition. The quantities $G_{kl,nm}$ in Eq. (25) determine the coupling between the single-particle intersubband excitations. If we neglect such coupling, then we get that the eigenfrequencies of the electron system are equal to the single-particle intersubband transition frequencies ω_{nm}. The expression for $G_{kl,nm}$, Eq. (26), consists of two terms. They describe the so-called depolarization and excitonic shifts, respectively.[5,6]

The system of equations (25) determine the longitudinal collective mode frequencies of the 2D electron gas confined in an arbitrary one-dimensional potential well. If the potential well is symmetrical, then the system of equations (25) splits into two independent systems. It is due to the fact that $G_{kl,nm}=0$ if $k+l+n+m$ is an odd number. These two systems describe the coupling of single-particle intersubband excitations between the states with different and the same parities and the conditions of the existence of their nontrivial solutions gives the equations for odd and even collective mode frequencies, respectively.

Figure 2 shows the dependences of odd and even longitudinal collective mode frequencies on the film thickness, calculated for $r_s(\bar{n})=4$. At first we note that the number of the collective modes at some film thickness is equal to the number of different single-particle intersubband excitations with energies $\hbar\omega_{nm}$. In the linear-optical regime such excitations are possible between the subbands from which at least one is occupied in the ground state. Therefore the number of collective modes stepwise increases at film thicknesses where new occupied subbands or new empty subbands at the top of the potential well appear. The former thicknesses are denoted in Figs. 1 and 2 by the vertical dashed lines and the latter thicknesses can be easily extracted from Fig. 1. In our calculations we take into account a new empty subband at the top of the potential well when its bottom energy ε_n becomes less than -0.05 eV. The dependences of the collective mode frequencies shown in Fig. 2 have discontinuities at film thicknesses where new subbands appear at the top of the potential well. These discontinuities arise from our approximation; we neglect electron transitions to the states of the continuous spectrum. It is seen that the discontinuities are absent for the collective modes with energies that lie below the continuum threshold. The inset in Fig. 2(a) shows that the collective modes are nondegenerate; i.e., there are no odd or even collective modes with the same energy.

The horizontal dashed lines in Fig. 2 mark two characteristic frequencies. One of them is the bulk plasma frequency $\omega_p=(4\pi\bar{n}e^2/m)^{1/2}$. It is seen that there are no collective modes with frequencies that lie far above the bulk plasma frequency. Also it is seen that a group of collective modes with frequencies near ω_p is formed with increasing film thickness. The frequencies of the collective modes from this group depend weakly on film thickness and the number of collective modes in this group increases with increasing film thickness. These collective modes can be interpreted as the standing plasma waves in thin metal slab.[13,21] Another frequency marked in Fig. 2 corresponds to the so-called multipole surface plasmon. The existence of the multipole plasmon at metal surfaces was demonstrated both experimentally and theoretically.[22] The frequency of the multipole surface plasmon is close to $0.8\omega_p$. However, here we use the value $0.85\omega_p$ that was given in the recent work of Barman *et al.*[23] and which is somewhat higher than the generally accepted value $0.8\omega_p$. It is seen from Fig. 2 that almost everywhere in

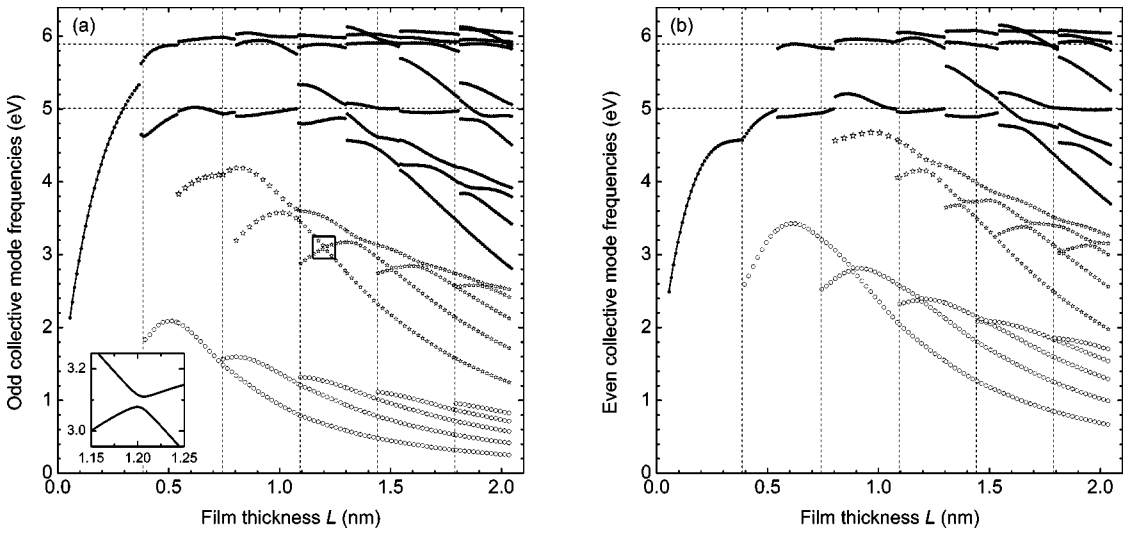

FIG. 2. Frequencies of odd (a) and even (b) longitudinal collective modes vs metal film thickness for $r_s(\overline{n})=4$. The vertical dashed lines denote the film thicknesses at which new occupied subbands appear. Two horizontal dashed lines mark the bulk plasma frequency ω_p and the frequency of the multipole surface plasmon, $0.85\omega_p$. The inset shows the region of two closely spaced collective mode frequencies in an expanded scale.

the range of film thickness from 0.5 to 2 nm there are both odd and even collective modes with frequencies which are close to $0.85\omega_p$.

The odd (even) longitudinal collective modes denoted by the open circles and stars in Fig. 2 arise from the coupling of the single-particle excitations with energies $\hbar\omega_{nm}$ such that $n-m=1$ $(n-m=2)$ and $n-m=3$ $(n-m=4)$, respectively. In order to illustrate it we plot in Fig. 3 the results of the model calculation in which we take into account only the single-particle excitations with energies $\hbar\omega_{nm}$ such that $n-m=1$. In this simulation the other single-particle excitations are considered as *forbidden*; i.e., we assume that the matrix elements $X_{nm}=0$ if $n-m\neq 1$. It is clear that in this case the number of collective modes at some film thickness is equal to the number of occupied subbands, N, in the ground state. It is seen from Fig. 3 that the coupling of N single-particle excitations with energies $\varepsilon_{n+1}-\varepsilon_n$ yields (i) $N-1$ collective modes with frequencies that almost coincide with the frequencies of collective modes denoted by the open circle in Fig. 2(a) and (ii) one collective mode with frequency that tends to the bulk plasma frequency ω_p with increasing film thickness. The latter result will be discussed in detail in Sec. VII.

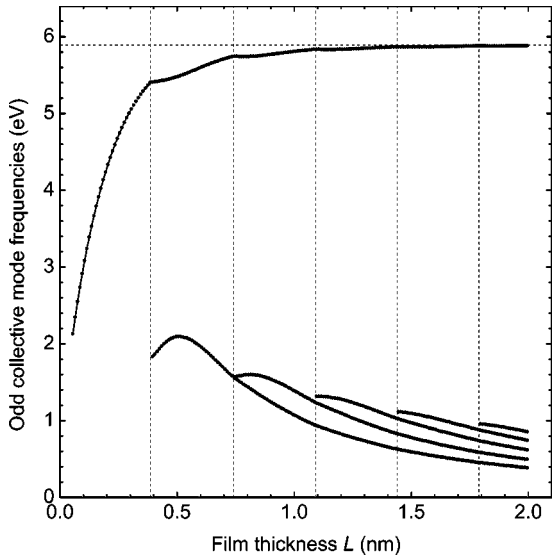

FIG. 3. Frequencies of odd longitudinal collective modes vs film thickness for $r_s(\overline{n})=4$. The vertical dashed lines denote film thicknesses at which new occupied subbands appear. The horizontal dashed line marks the bulk plasma frequency ω_p. The collective mode frequencies are calculated on the model assumption that the intersubband transitions are allowed only between adjacent subbands.

IV. REFLECTION, TRANSMISSION, AND ABSORPTION SPECTRA

We will further discuss the linear-optical properties of thin metal films and illustrate them in an example of metal film with thickness $L=1$ nm and mean electron density $\overline{n}$ characterized by Wigner-Seitz radius $r_s(\overline{n})=4$. In order to give an idea of the metal film with such parameters we plot in Fig. 4 the self-consistent potentials, eigenenergies, and density distributions. It is seen from Fig. 4(a) that the effective potential $e\varphi_0+V_0$ is formed mainly by the exchange-correlation potential V_0. Figure 4(b) shows that in such film there are six energy subbands and three of them are occupied. The electron density n_0 in Fig. 4(c) exhibits characteristic Friedel oscillations. A detailed analysis of the self-consistent potentials and density distributions as functions of L and $\overline{n}$ was done by Schulte.[24]

We start the analysis of the linear-optical properties of thin metal films from the discussion of absorption spectra. Figure 5 shows the spectral dependence of the absorption

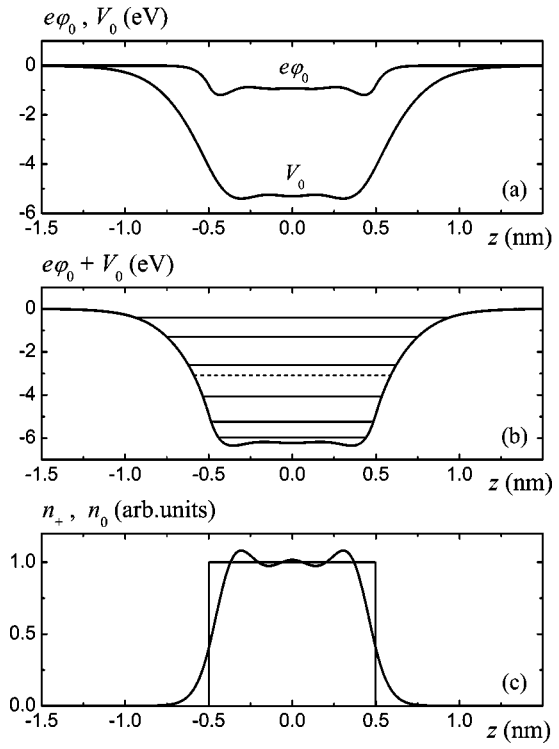

FIG. 4. (a) Electrostatic $e\varphi_0$ and exchange-correlation V_0 potentials, (b) effective potential $e\varphi_0+V_0$, Kohn-Sham eigenenergies ε_n (solid lines) and Fermi energy ε_F (dashed line), and (c) background n_+ and electron n_0 densities for metal film with the thickness $L=1$ nm and $r_s(\overline{n})=4$.

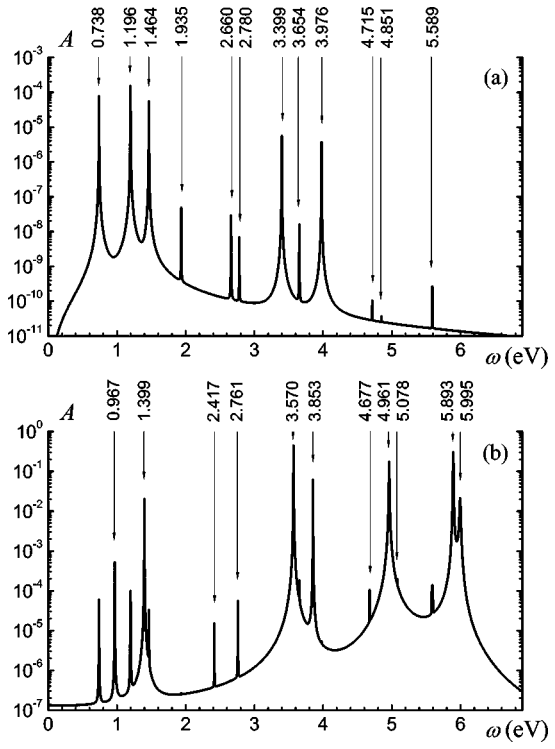

FIG. 5. Absorption spectrum for normal incidence (a) and incidence of *p*-polarized waves at the angle $\theta=30°$ (b). The vertical arrows denote the transverse (a) and longitudinal (b) collective mode frequencies. The relaxation time $\tau=1$ ps.

coefficient A for two different cases of incident waves. The absorption coefficient is defined as $A=1-R-T$, where R and T are the intensity reflection and transmission coefficients. We assume here that the relaxation time τ is equal to 1 ps unless otherwise specified.

In the case of normal incidence of light waves on the metal film the absorption spectrum is shown in Fig. 5(a). It contains the resonant peaks corresponding to the transverse collective mode excitations. The frequencies of transverse collective modes are shown in Fig. 5(a) by the vertical arrows and they almost coincide with the intersubband transition frequencies ω_{nm}. The shift between the collective mode frequencies and ω_{nm} is only about 10^{-5} eV, which is significantly smaller than the characteristic absorption linewidth.[3] The absorption peaks in Fig. 5(a) differ in their amplitudes. One of the reasons for this difference is connected with the parity of the collective modes. The amplitudes of peaks corresponding to excitations of odd modes (for example, the first three low-frequency resonances) are significantly larger than those corresponding to excitations of even modes (for example, the second three low-frequency resonances). The frequencies of odd and even transverse collective modes are close to the transition frequencies ω_{nm} between the Kohn-Sham eigenstates Φ_n with different and the same parity, respectively.

In the case of *s*-polarized incident waves the absorption spectrum also contains resonant peaks corresponding to transverse collective mode excitations. The deviation from normal incidence does not result in any qualitative changes of the absorption spectrum. On the contrary, in the case of *p*-polarized incident waves the absorption spectrum contains resonant peaks corresponding to excitations of both transverse and longitudinal collective modes. Here, it should be noted that *p*-polarized incident waves cannot excite purely longitudinal or transverse collective modes. Strictly speaking *p*-polarized incident waves can excite the longitudinal-transverse collective modes. Nevertheless, we will refer to different excitations as longitudinal or transverse collective mode excitations because there are a number of features which allow us to discern them.

Figure 5(b) shows the absorption spectrum for the case of *p*-polarized incident waves at the angle $\theta=30°$. The vertical arrows denote the longitudinal collective mode frequencies. Here, it is necessary to note that there is a weak dependence of the collective mode frequencies on the angle of incidence, θ. Below we will discuss these dependences in detail. In order to avoid confusion we arrange to refer to collective modes by values of their frequencies in the limit $\theta=0$. It is seen from Fig. 5(b) that the amplitudes of some absorption peaks corresponding to excitations of the longitudinal modes (for example, peaks at frequencies 3.57 eV or 4.961 eV) are significantly larger than those corresponding to excitations of the transverse modes. The maximum collective mode frequency is 5.995 eV and it is only slightly larger than the bulk plasma frequency $\omega_p=5.891$ eV, which characterizes the collective excitation (volume plasmon) in infinite electron

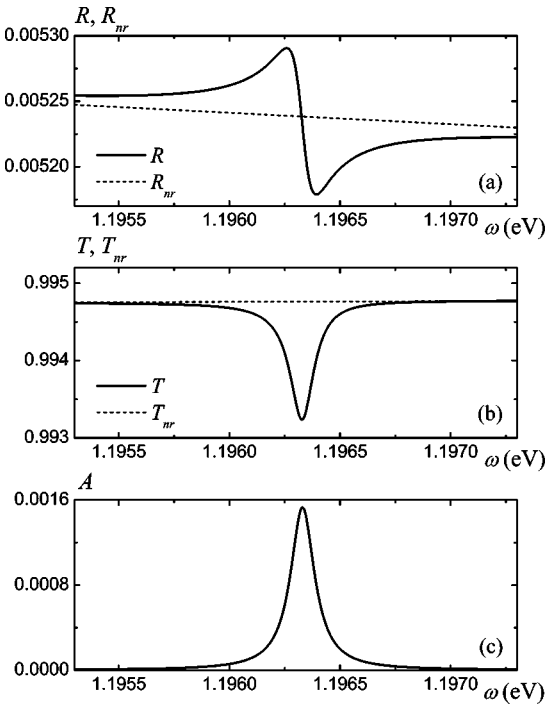

FIG. 6. Spectral dependence of reflection R (a), transmission T (b), and absorption A (c) coefficients as well as nonresonant reflection R_{nr} (a) and transmission T_{nr} (b) coefficients for the case of normal incidence. The field frequency ω varies in the vicinity of the intersubband transition frequency $\omega_{32}=1.1963$ eV; the relaxation time $\tau=10$ ps.

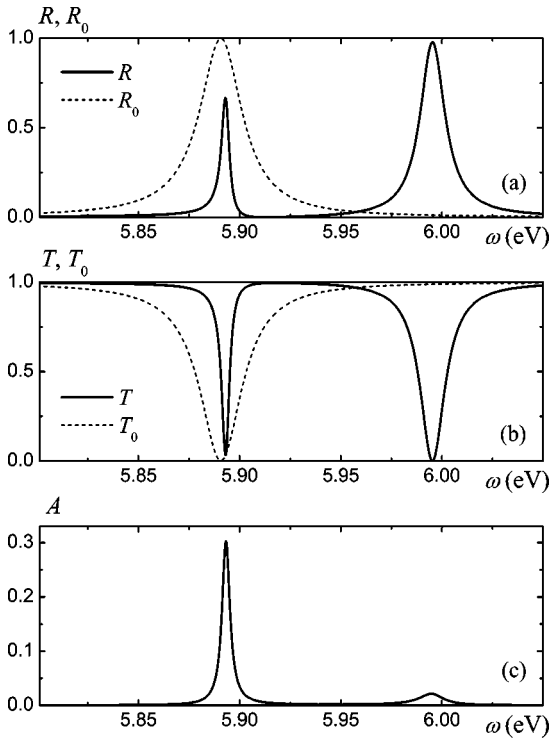

FIG. 7. Spectral dependence of reflection R (a), transmission T (b), and absorption A (c) coefficients for p-polarized incident waves at $\theta=30°$. Reflection R_0 (a) and transmission T_0 (b) coefficients are calculated with the help of the Fresnel formulas. The field frequency ω varies in the vicinity of two closely spaced longitudinal collective mode frequencies 5.893 eV and 5.995 eV. The bulk plasma frequency $\omega_p=5.891$ eV; the relaxation time $\tau=1$ ps.

gas of a given density. This result is in agreement with previous calculations.[13]

For the case of normal incidence, Fig. 6 shows dependences of reflection R, transmission T, and absorption A coefficients on field frequency varying in the vicinity of the intersubband transition frequency $\omega_{32}=1.1963$ eV. In Fig. 6 we also plot nonresonant reflection R_{nr} and transmission T_{nr} coefficients that are calculated in an approximation of the local response. This approximation does not take into account the nonlocal resonant response of the valence electrons; namely, it neglects the right-hand part of Eq. (18). It is seen from Fig. 6(c) that the amplitude of the absorption resonance corresponding to excitation of the transverse collective mode is quite small, even for the relatively large relaxation time $\tau=10$ ps that is used here. The resonant deviations of the reflection and transmission coefficients from the nonresonant background are also small. In other words the resonant part of the field response of the metal film is significantly smaller than the nonresonant part. But it does not mean that in the case under consideration the resonant part of the current density is also significantly smaller than the nonresonant part. In fact, they are comparable, but at the same time there is an important distinction between them. The sign of the resonant current density changes 3 times across the metal film while the sign of the nonresonant current density does not change.

Figure 7 shows reflection R, transmission T, and absorption A coefficients of p-polarized incident waves at the angle $\theta=30°$ as functions of field frequency varying in the vicinity of two closely spaced longitudinal collective mode frequencies 5.893 eV and 5.995 eV. It is seen that the reflection, transmission, and absorption coefficients change greatly near the collective mode frequencies. For comparison, in Fig. 7 we also plot reflection R_0 and transmission T_0 coefficients, which are calculated using the Fresnel formulas for metal film with the dielectric permittivity that is given by Eq. (16). It is known that the dependences of the reflection R_0 and transmission T_0 coefficients on the field frequency have only two specific points. One of them takes place at a frequency when the angle of incidence θ becomes equal to Brewster's angle (in our case this frequency is 7.215 eV). The other specific point that is just shown in Fig. 7 appears at the bulk plasma frequency $\omega_p=5.891$ eV.

V. FIELD DISTRIBUTION

In this section we discuss the field and induced charge density distributions for the case of a p-polarized wave that is incident on the metal film at the angle $\theta=30°$. Figure 8 shows moduli of the complex amplitudes of the tangential and normal components of the vector potential as well as induced charge density for three different values of field frequency. The first case is shown in Figs. 8(a)–8(c) and it is an example of a nonresonant interaction of electromagnetic waves with the metal film. The field frequency is equal to 0.5 eV and it does not coincide with any collective mode fre-

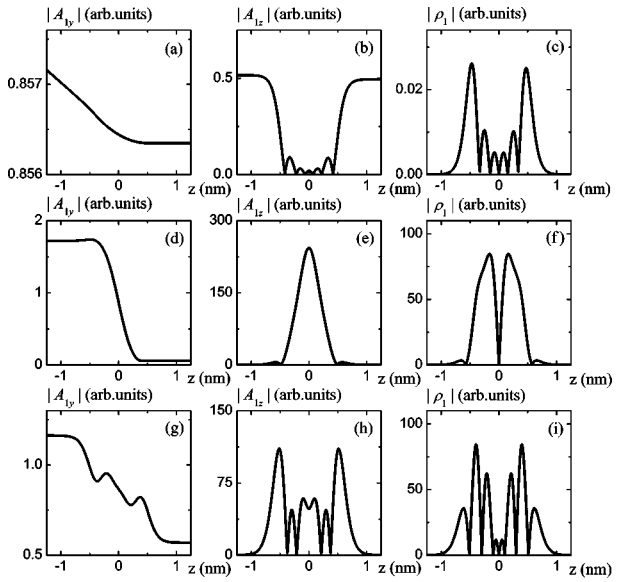

FIG. 8. Moduli of complex amplitudes of the tangential (a), (d), (g) and normal (b), (e), (h) components of the vector potential as well as induced charge density (c), (f), (i) as functions of transversal coordinate z for the case of p-polarized incident wave at $\theta=30°$. The field frequency ω is equal to 0.5 eV (a)–(c), 5.995 eV (d)–(f), and 3.57 eV (g)–(i). The relaxation time $\tau=1$ ps.

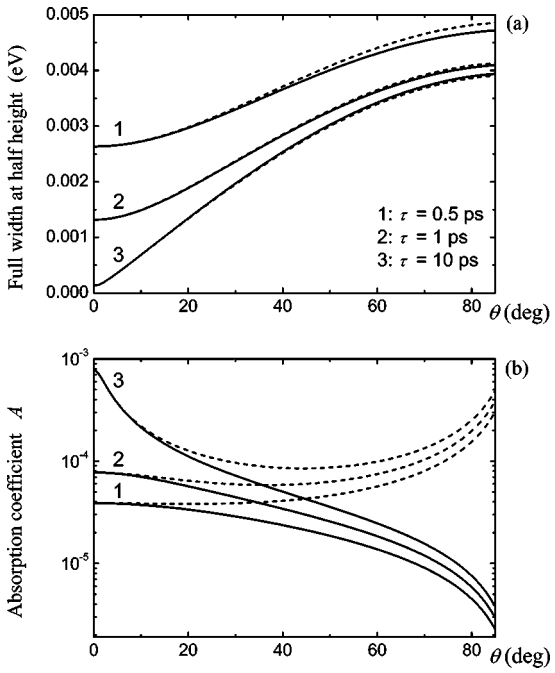

FIG. 9. Angular dependence of the full width at half height (a) and height (b) of the absorption peak at the frequency 0.738 eV. The incident wave is s polarized (solid curves) and p polarized (dashed curves). The relaxation time τ is equal to 0.5 ps (1), 1 ps (2), and 10 ps (3).

quency. In two other cases the field frequency is equal to longitudinal collective mode frequencies 5.995 eV and 3.57 eV and these cases are shown in Figs. 8(d)–8(f) and 8(g)–8(i), respectively.

In the nonresonant case the tangential component of the vector potential varies slightly within the metal film. The electromagnetic field on the left side of the metal film, where the electron density vanishes, is a superposition of the incident and reflected waves. Its amplitude is an oscillating function of the transverse coordinate z. The frequency of these oscillations is equal to the double normal component of the wave vector of the incident wave. Certainly, we cannot see these oscillations on the nanometer scale, but we see in Fig. 8(a) that the amplitude changes on the left of the metal film. The amplitude of field on the right side of the metal film is constant and equal to the amplitude of the transmitted wave. It is seen from Fig. 8(b) that the normal component of the vector potential varies significantly within the metal film as opposed to the tangential component. The variation of the normal component of the field can be qualitatively understood with the help of the well-known boundary conditions for macroscopic field quantities. The normal component of the electric displacement vector is continuous at the boundary of the media. The dielectric permittivity of free electron gas at the considered field frequency can be evaluated as 10^2. Hence, the amplitude of the normal component of the vector potential inside the metal film has to decrease approximately by a factor of 10^2. Such decreasing and oscillations of the normal component of the field are seen in Fig. 8(b). Also we note here that in the nonresonant case the induced charge density is maximized approximately at the boundaries of the metal film.

As is seen from Figs. 8(d)–8(i) the field and induced charge density distributions undergo drastic changes under conditions of the longitudinal collective excitations. The amplitude of the normal component of the field inside the metal film significantly increases and can be two orders of magnitude larger than the amplitude of the incident wave. The induced charge density also increases and can significantly extend beyond the nominal boundaries of the metal film at $z=\pm L/2$.

VI. ANGULAR DEPENDENCES OF THE OPTICAL RESPONSE

A. Transverse collective excitations

We now discuss the angular dependence of the optical response of thin metal films under the conditions of transverse collective mode excitations. As an example, we consider the absorption peak at the frequency 0.738 eV (see Fig. 5). In general, every absorption peak can be characterized by its position, width, and height. We determine the width of the absorption peaks at half height. The positions of the absorption peaks corresponding to the transverse collective mode excitations are almost constant. The difference between positions of these peaks and intersubband transition frequencies ω_{nm} amounts to about 10^{-5} eV, which is much smaller than the characteristic width of absorption peaks. Figure 9 shows the width and height of the absorption peak at the frequency 0.738 eV as functions of the angle of incidence, θ, which are calculated for three different relaxation times τ and two mutually orthogonal polarizations of the incident wave. In the case of normal incidence $\theta=0$, the broadening of the ab-

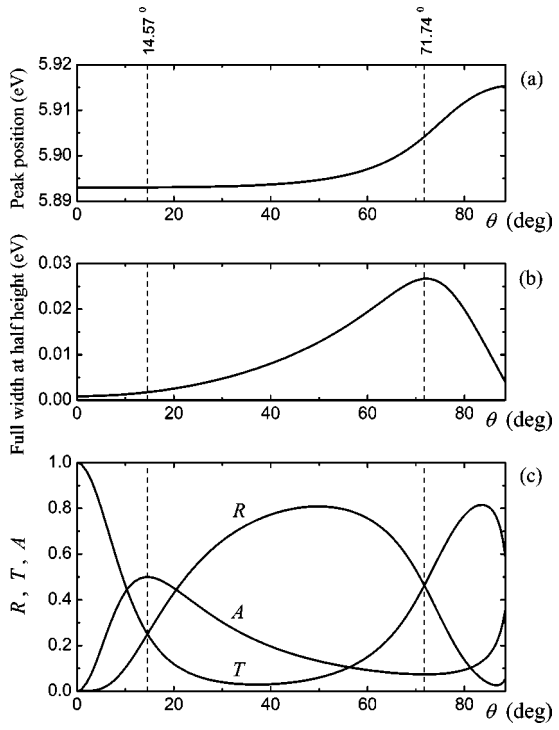

FIG. 10. Angular dependence of position (a), full width at half height (b), and height (c) of the absorption peak corresponding to excitation of one of the longitudinal collective modes. The height of the absorption peak is determined by the absorption coefficient A. In addition to the absorption coefficient A, the related reflection R and transmission T coefficients ($R+T+A=1$) are also plotted in the bottom panel. The incident wave is p polarized. The vertical dashed lines denote the positions of extrema of the absorption coefficient A. The relaxation time $\tau=1$ ps.

sorption peak is absent, the width of the absorption peak is equal to $2/\tau$, and the height of the absorption peak is proportional to the relaxation time. With increasing angle of incidence there is a broadening of the absorption peak, which is more pronounced for longer relaxation time. The broadening for mutually orthogonal polarizations of incident waves almost coincides but at the same time there is a quite observable difference. Also, it is seen from Fig. 9(b) that the dependences of the height of the absorption peak on the angle of incidence in the cases of s- and p-polarized incident waves are significantly different.

B. Longitudinal collective excitations

In this subsection we discuss the angular dependence of the optical response of thin metal films under the conditions of longitudinal collective mode excitations. At first, we consider the absorption peak corresponding to excitation of one of the longitudinal collective modes. Figure 10 shows the position, full width at half height, and height of the absorption peak as functions of the angle of incidence, θ. It is seen that the position of the absorption peak shifts with increasing angle of incidence. This shift amounts to about 10^{-2} eV. Most of the absorption peaks have ultraviolet shifts as is seen in Fig. 10(a). An infrared shift may occur in the cases when there are two or more closely spaced absorption peaks.

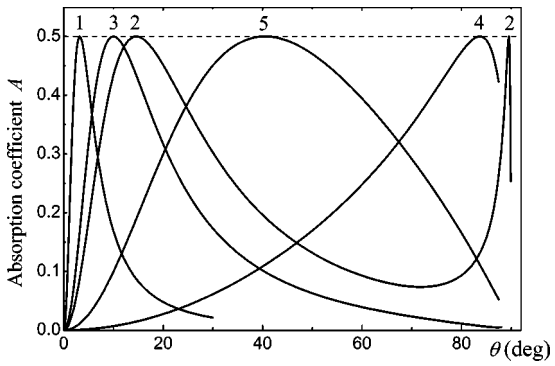

FIG. 11. Angular dependence of heights of the absorption peaks corresponding to the excitations of the longitudinal collective modes. Frequencies of the collective modes tend to 5.995 eV (1), 5.893 eV (2), 4.961 eV (3), 3.853 eV (4), and 3.57 eV (5) in the limit $\theta=0$. The incident wave is p polarized; the relaxation time $\tau=1$ ps.

In Fig. 10 two vertical dashed lines denote positions of extrema of the absorption coefficient A. The optical response at these two points has a few specific features. The absorption coefficient at the angle of incidence, $\theta=71.74°$, has the local minimum and the reflection and transmission coefficients equal to each other and the width of the absorption peak reaches the maximum. The absorption coefficient at the angle of incidence, $\theta=14.57°$, reaches the absolute maximum and is equal to 0.5. At the latter point the reflection and transmission coefficients are equal to 0.25. Also, we notice here without illustration that at the latter point the width of the absorption peak is exactly 2 times larger than in the limit $\theta=0$. We have found similar points with the mentioned properties for a number of other collective excitations.

Figure 11 shows the angular dependence of the absorption coefficient under the conditions of resonant excitations of odd longitudinal collective modes. It is seen that the absorption coefficient does not exceed the value 0.5. It means that metal film cannot absorb more than half of the energy flux of incident waves under the mentioned conditions. The height of the absorption peak near the frequency 5.893 eV reaches the absolute maximum twice. In general, one can notice that the height of the absorption peaks at smaller frequencies reaches the absolute maximum later with increasing angle of incidence.

Now we consider the question why the absorption coefficient cannot be greater than 0.5 under the conditions of odd collective mode excitations. At first we note that under these conditions the optical response of the metal film is mainly formed by the normal component of the current density and induced charge density. These quantities significantly increase and they are even and odd functions of the transversal coordinate z, respectively. Using only this fact it is easy to show that the reflection and transmission coefficients can be represented as

$$R=|r|^2, \quad T=|1-r|^2, \tag{27}$$

where the complex number $r=r_1+ir_2$ characterizes the linear-optical response of the metal film. By substituting

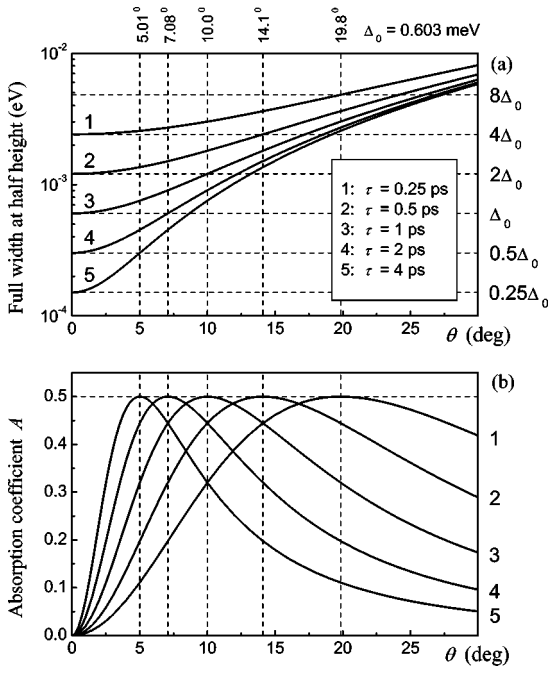

FIG. 12. Angular dependence of the full width at half height (a) and height (b) of the absorption peak corresponding to excitation of the longitudinal collective mode. The dependences are calculated for five different relaxation times τ. The frequency of the collective mode tends to 4.961 eV in the limit $\theta=0$. The incident wave is p polarized. The vertical dashed lines denote the positions of extrema of the absorption coefficient A.

these expressions into the energy conservation equation $R+T+A=1$ we get

$$\left(r_1-\frac{1}{2}\right)^2+r_2^2=\frac{1}{2}\left(\frac{1}{2}-A\right). \tag{28}$$

It is seen that a solution of Eq. (28) exists only if the absorption coefficient is less than or equal to 0.5. Moreover, if the absorption coefficient is equal to 0.5, then the reflection and transmission coefficients are equal to 0.25.

Finally we discuss how the resonant response of thin metal films depends on the transverse relaxation time τ. As an example we consider the absorption peak near the frequency 4.961 eV. Figure 12 shows the angular dependence of the full width at half height and height of the absorption peak for different values of the relaxation time τ. It is seen that the full width at half height is inversely proportional to the relaxation time only in the limit $\theta=0$. We have already mentioned that the width of the absorption peak at the angle of incidence where the absorption coefficient reaches the maximum is 2 times larger than that in the limit $\theta=0$. This fact is shown in Fig. 12(a) with the help of the horizontal dashed lines. As far as the absorption coefficient is concerned, the longer the relaxation time, the smaller the angle of incidence where the absorption coefficient reaches the absolute maximum.

VII. TRANSITION FROM 2D TO 3D SYSTEMS

In the rest of this paper we consider the solution of Eq. (25) in the asymptotic limit $L\to\infty$. Our aim is to obtain from Eq. (25) the dispersion relation for longitudinal plasma waves in an infinite electron gas. For the sake of simplicity we consider this problem in the random phase approximation, neglecting exchange and correlation effects. At first among all possible intersubband transitions we select such transitions from the m to n subbands that $n-m=p$. The integer number p will be defined later. We consider all other, nonselected by us, intersubband transitions as *forbidden*. In accordance with it we can introduce the quantities X_m and G_{lm} in the following way:

$$X_{nm}=\begin{cases} X_m, & n=m+p, \\ 0, & n\neq m+p, \end{cases} \tag{29}$$

$$G_{kl,nm}=\begin{cases} G_{lm}, & k=l+p\cap n=m+p, \\ 0, & k\neq l+p\cup n\neq m+p. \end{cases} \tag{30}$$

The selection of a certain group of intersubband transitions from all possible ones is an approximation if the film thickness L is finite. But in the limit $L\to\infty$ the given selection will be served automatically by the momentum conservation law. To evaluate the matrix elements G_{lm} we take the single-particle wave functions

$$\Phi_n=\sqrt{\frac{2}{L}}\sin\left(\frac{\pi nz}{L}\right), \quad n=1,2,\ldots, \tag{31}$$

which describe the motion of electrons in the rectangular potential well with infinitely high barriers. The longitudinal collective excitations in such a potential well were studied in Ref. 25. Substitution of Eq. (31) into Eq. (26) with subsequent integration gives

$$G_{lm}=\frac{e^2}{\pi m_e}\left(\frac{\pi}{L}\right)^3[(2l+p)(2m+p)+p^2\delta_{lm}]r_m, \tag{32}$$

where δ_{lm} is the Kronecker symbol,

$$r_m=\begin{cases} 1, & m<N-p, \\ \dfrac{N^2-m^2}{p(2m+p)}, & N-p\leqslant m\leqslant N, \end{cases} \tag{33}$$

and N is the number of occupied subbands. Using Eqs. (29), (30), and (32), we can rewrite Eq. (25) in the matrix form

$$(\mathbf{A}+\mathbf{B})\mathbf{X}=\omega^2\mathbf{X}, \tag{34}$$

where $\mathbf{X}$ is the N-dimensional vector with elements X_m; $\mathbf{A}$ and $\mathbf{B}$ are the square matrixes with elements

$$A_{lm}=\frac{e^2}{\pi m_e}\left(\frac{\pi}{L}\right)^3(2l+p)(2m+p)r_m, \tag{35}$$

$$B_{lm}=\frac{e^2}{\pi m_e}\left(\frac{\pi}{L}\right)^3p^2\left(r_m+\frac{\pi^2a_B}{4L}(2m+p)^2\right)\delta_{lm}, \tag{36}$$

where a_B is the Bohr radius. The nontrivial solution of Eq. (34) exists on condition that

$$\det[\mathbf{A}+\mathbf{B}-\omega^2\mathbf{I}]=0, \tag{37}$$

where $\mathbf{I}$ is the identity matrix. The solution of Eq. (37) gives the eigenvalues ω_n^2. If we neglect the matrix $\mathbf{B}$ in Eq. (37), then we get that all eigenvalues ω_n^2 are equal to zero except for one eigenvalue which is equal to the trace of the matrix $\mathbf{A}$ (see the Appendix). Let us denote this eigenvalue as Ω^2. Taking into account the matrix $\mathbf{B}$ in Eq. (37) gives corrections to Ω^2. In the limit $L\to\infty$ these corrections are small and describe the effects of the nonlocal interaction of the electromagnetic field with the homogeneous electron gas. They can be considered within the perturbation theory. In the Appendix we obtain the first-order correction to Ω^2 due to the matrix $\mathbf{B}$ and the result is

$$\Omega^2=\mathrm{Tr}(\mathbf{A})+\frac{\mathrm{Tr}(\mathbf{AB})}{\mathrm{Tr}(\mathbf{A})}+\cdots. \tag{38}$$

In the limit $L\to\infty$ we have to set $\pi N/L=k_F$ and $\pi p/L=q$, where q is the wave vector of the electromagnetic field. The latter equality is due to momentum conservation. As a result we get the dispersion relation

$$\Omega^2=\omega_p^2\left(1+\frac{9\pi a_B k_F}{20}\left(\frac{q}{k_F}\right)^2+\cdots\right), \tag{39}$$

which exactly coincides, up to second order in q/k_F, with that for longitudinal plasma waves in an infinite electron gas.[26]

VIII. CONCLUSIONS

The linear-optical properties of unbacked thin metal films have been studied within the jellium model and the time-dependent density-functional approach. Most previous works consider the interaction of thin metal film (2D electron gas) with an electric field perpendicular to the surface of the film. The electric field component parallel to the surface of the film is usually neglected. In the present work, we have treated both perpendicular and parallel components of the electromagnetic field microscopically and the results are performed in terms of strictly calculated reflection, transmission, and absorption coefficients.

We have analyzed the absorption spectra of thin metal films. In the case of *s*-polarized incident waves the absorption spectrum contains resonant peaks corresponding to excitations of the transverse collective modes. The frequencies of the transverse collective modes almost coincide with the single-particle intersubband transition frequencies ω_{nm}. In the case of *p*-polarized incident waves the absorption spectrum contains resonant peaks corresponding to excitations of both transverse and longitudinal collective modes. The most intense absorption resonances correspond to excitations of odd longitudinal collective modes. It has been shown that there are no collective modes with frequencies that lie far above the bulk plasma frequency ω_p. Also, it has been shown that the reflection and transmission coefficients of the metal film change greatly near the frequencies of the longitudinal collective excitations.

The analysis of the field distribution has shown that under the conditions of longitudinal collective mode excitations the amplitude of the normal component of the field inside the metal film significantly increases and can be more than two orders of magnitude larger than the amplitude of the incident wave.

We have shown that the linear-optical response of thin metal films under the conditions of longitudinal collective mode excitations has a few specific features. For example, metal film cannot absorb more than a half of energy flux of the incident wave. At the angle of incidence, where absorption reaches the absolute maximum, the reflection and transmission coefficients are equal to one-fourth and the width of the absorption peak is 2 times larger than that in the limit $\theta=0$. These features are reproduced in the same way for different collective mode excitations.

We have analyzed the dependences of the longitudinal collective mode frequencies on the metal film thickness. It was shown that (i) with increasing film thickness a group of collective modes with frequencies near ω_p appears and these modes can be interpreted as the standing plasma waves in a thin slab. (ii) In a thin slab there exists a couple of collective modes which correspond to the multipole surface-plasmon mode. (iii) Some collective excitations can arise from the effective coupling between the single-particle intersubband excitations belonging to a certain group. Also, we have shown analytically how the longitudinal collective excitations transform under the transition from two- to three-dimensional electron systems. Starting from the eigenvalue problem (25) which determines the frequencies of the longitudinal collective mode in 2D electron systems, we have obtained in the limit $L\to\infty$ the well-known dispersion relation (39) for longitudinal plasma waves in an infinite electron gas. For the sake of simplicity this problem was considered in the random phase approximation.

ACKNOWLEDGMENTS

This work was supported in part by the Russian Foundation for Basic Research (Grant No. 02-02-17138), ''Universities of Russia'' Program (Grant No. UR.01.03.001), and ISTC Project No. 2651.

APPENDIX

Let us have an $N\times N$ matrix $\mathbf{C}$ that can be performed as a sum of two matrices,

$$\mathbf{C}=\mathbf{A}+\mu\mathbf{B}, \tag{A1}$$

with elements

$$A_{nm}=f(n)g(m), \quad B_{nm}=h(n)\delta_{nm}, \tag{A2}$$

where $f(n)$, $g(n)$, $h(n)$ are arbitrary functions and μ is the scalar parameter. One can show that all eigenvalues of the matrix $\mathbf{A}$ are equal to zero except for one and this eigenvalue is equal to the trace of the matrix. Eigenvalues of the matrix $\mathbf{B}$ are simply equal to its diagonal elements $h(n)$. The sub-

ject of our interest is the eigenvalues λ_n of the matrix **C**. If μ is a small parameter, then the eigenvalues λ_n can be calculated within the perturbation theory. Below we obtain the first-order correction to the eigenvalue λ_1, which is only nonzero in the limit $\mu=0$. The eigenvalues λ_n of the matrix **C** are roots of the characteristic equation

$$\lambda^N-\sum_{n=1}^{N}(A_{nn}+\mu B_{nn})\lambda^{N-1} + \frac{1}{2}\sum_{\substack{m,n=1\\ m\neq n}}^{N}\mu B_{mm}(2A_{nn}+\mu B_{nn})\lambda^{N-2}+\cdots=0. \quad \text{(A3)}$$

Within the perturbation theory the eigenvalue λ_1 can be expanded into a power series

$$\lambda_1=\mathrm{Tr}(\mathbf{A})+\sum_{m=1}^{\infty}\mu^m x_m. \quad \text{(A4)}$$

By substituting Eq. (A4) into Eq. (A3) and collecting terms with the same powers of μ, one can get

$$\mathrm{Tr}(\mathbf{A})x_1=\mathrm{Tr}(\mathbf{AB}). \quad \text{(A5)}$$

So the final result is

$$\lambda_1=\mathrm{Tr}(\mathbf{A})+\mu\frac{\mathrm{Tr}(\mathbf{AB})}{\mathrm{Tr}(\mathbf{A})}+\cdots. \quad \text{(A6)}$$

*Electronic address: andreev@sr1.phys.msu.su

[1] T. Ando, A.B. Fowler, and F. Stern, Rev. Mod. Phys. **54**, 437 (1982).
[2] See, for example, S. Das Sarma and I.K. Marmorkos, Phys. Rev. B **47**, 16 343 (1993), and references therein.
[3] D.A. Dahl and L.J. Sham, Phys. Rev. B **16**, 651 (1977).
[4] W.P. Chen, Y.J. Chen, and E. Burstein, Surf. Sci. **58**, 263 (1976).
[5] S.J. Allen, D.C. Tsui, and B. Vinter, Solid State Commun. **20**, 425 (1976).
[6] T. Ando, Z. Phys. B **26**, 263 (1977).
[7] See, for example, S. Tsujino, M. Rufenacht, H. Nakajima, T. Noda, C. Metzner, and H. Sakaki, Phys. Rev. B **62**, 1560 (2000); I. Shtrichman, C. Metzner, E. Ehrenfreund, D. Gershoni, K.D. Maranowski, and A.C. Gossard, *ibid.* **65**, 035310 (2001).
[8] S. Das Sarma, Phys. Rev. B **29**, 2334 (1984).
[9] M. Kaloudis, K. Ensslin, A. Wixforth, M. Sundaram, J.H. English, and A.C. Gossard, Phys. Rev. B **46**, 12 469 (1992).
[10] P. Hohenberg and W. Kohn, Phys. Rev. **136**, B864 (1964).
[11] W. Kohn and L.J. Sham, Phys. Rev. **140**, A1133 (1965).
[12] J.F. Dobson, Phys. Rev. B **46**, 10 163 (1992).
[13] W.L. Schaich and J.F. Dobson, Phys. Rev. B **49**, 14 700 (1994).
[14] T.K. Ng, Phys. Rev. Lett. **62**, 2417 (1989).
[15] G. Vignale and W. Kohn, Phys. Rev. Lett. **77**, 2037 (1996).
[16] G. Vignale, C.A. Ullrich, and S. Conti, Phys. Rev. Lett. **79**, 4878 (1997).
[17] N.D. Lang and W. Kohn, Phys. Rev. B **1**, 4555 (1970).
[18] A. Zangwill and P. Soven, Phys. Rev. A **21**, 1561 (1980).
[19] M.J. Stott and E. Zaremba, Phys. Rev. A **21**, 12 (1980).
[20] C.A. Ullrich and G. Vignale, Phys. Rev. B **58**, 15 756 (1998).
[21] O. Heinonen and W. Kohn, Phys. Rev. B **48**, 12 240 (1993).
[22] K.-D. Tsuei, E.W. Plummer, A. Liebsch, K. Kempa, and P. Bakshi, Phys. Rev. Lett. **64**, 44 (1990), and references therein.
[23] S.R. Barman, C. Stampfl, P. Häberle, W. Ibañez, Y.Q. Cai, and K. Horn, Phys. Rev. B **64**, 195410 (2001).
[24] F.K. Schulte, Surf. Sci. **55**, 427 (1976).
[25] W.H. Backes, F.M. Peeters, F. Brosens, and J.T. Devreese, Phys. Rev. B **45**, 8437 (1992).
[26] See, for example, S. Ichimaru, Rev. Mod. Phys. **54**, 1017 (1982).